Syntheses and Characterization of Dinuclear High-Spin Iron(II,III) and (III,III) Complexes with 2,6-Bis[bis(2-benzimidazolylmethyl)-aminomethyl]-4-methylphenolate(1−)

Masatatsu SUZUKI, Hiroki OSHIO,† Akira UEHARA,* Kazutoyo ENDO,††
Makoto YANAGA,†† Sigeo KIDA,† and Kazuo SAITO†††
Department of Chemistry, Faculty of Science, Kanazawa University, Kanazawa 920
†Coordination Chemistry Laboratories, Institute for Molecular Science, Okazaki 444
††Department of Chemistry, Faculty of Science, Tokyo Metropolitan University, Fukazawa, Setagaya, Tokyo 158
†††International Christian University, Osawa, Mitaka, Tokyo 181
(Received July 2, 1988)

Two types of dinuclear high-spin mixed valence iron(II,III) complexes, $[Fe_2(L\text{-}Bzim)(RCOO)_2](BF_4)_2\cdot nH_2O$ (RCOO=CH_3COO (**1**) or C_6H_5COO (**2**)), and $[Fe_2(L\text{-}Bzim)(C_6H_5COO)_2(OH)]BF_4\cdot H_2O$ (**3**), and dinuclear high-spin iron(III,III) complexes, $[Fe_2(L\text{-}Bzim)(CH_3COO)_2](ClO_4)_3\cdot 3.5H_2O$ (**4**) and $[Fe_2(L\text{-}py)(C_6H_5COO)_2](ClO_4)_3\cdot CH_3CN\cdot H_2O$ (**5**) were prepared, where L-Bzim is 2,6-bis[bis(2-benzimidazolylmethyl)aminomethyl]-4-methylphenolate(1−) and L-py is 2,6-bis[bis(2-pyridylmethyl)aminomethyl]-4-methylphenolate(1−). Mössbauer spectra of the mixed valence complexes revealed that they involve high-spin iron(II) and (III) ions in equimolar amount. Their ESR spectra exhibited a signal at g_{av}=1.7 near liquid helium temperature characteristic of an antiferromagnetically spin coupled high-spin iron(II,III) dimer. Magnetic susceptibility measurements over the temperature range 80—300 K revealed that weak antiferromagnetic spin-exchange interactions are present between iron(II) and iron(III) ions ($J\approx-5$ cm^{-1}). The complexes showed an intervalence absorption band in the near infrared region, indicating that they belong to class II mixed valence type on the classification of Robin and Day. Cyclic voltammogram of **3** in acetonitrile showed two sets of reversible redox couples at 0.00 and 0.66 V vs. SCE, which are assigned to the redox reactions of Fe(II,III)/Fe(II,II) and Fe(III,III)/Fe(II,III), respectively. The complexes **4** and **5** exhibited weak antiferromagnetic interaction (J=−9—−12 cm^{-1}). ESR spectra of **4** and **5** showed a significant temperature dependence.

Dinuclear mixed valence iron(II,III) centers have been found to exist in some iron proteins such as pink uteroferrin,[1-5] the reduced form of bovine spleen acid phosphatase,[1,2,6] and semi-methemerythrin.[7-9] Those iron proteins were characterized mainly by ESR spectroscopy. They exhibit an ESR signal at $g<2.0$, which was interpreted in terms of antiferromagnetic exchange interaction between high-spin iron(II) and high-spin iron(III) ions.

In the previous studies,[10,11] we reported preparation of the first examples of dinuclear high-spin iron(II, III) complexes with the dinucleating ligand 2,6-bis-[bis(2-benzimidazolylmethyl)aminomethyl]-4-methyl-phenolate(1−)=L-Bzim or 2,6-bis[bis(2-pyridylmethyl)-aminomethyl]-4-methylphenolate(1−)=L-py (Fig. 1). The L-py complexes were characterized by various spectroscopies such as ESR and Mössbauer. Recently Brovik and Que determined the crystal structure of $[Fe_2(L\text{-}py)(C_2H_5COO)_2](BPh_4)_2\cdot CH_3COCH_3$, where two irons are triply bridged by phenolato and two carboxylato groups.[12] It is interesting to investigate how the ligand environment influences physicochemical properties of mixed valence iron(II,III) complexes. As an extension of our current work on the mixed valence iron(II,III) complexes with various dinucleating ligands, we report here details of physicochemical properties of the iron(II,III) and (III,III) complexes with L-Bzim in comparison with those of the L-py complexes. Recently such dinuclear mixed valence complexes with three bridging ligands (two carboxylate ions and oxide or phenolate ion) have been reported by two groups.[13,14]

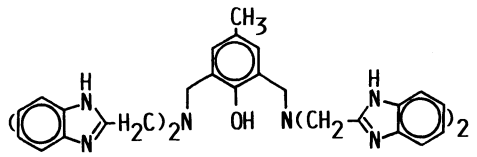

HL-Bzim

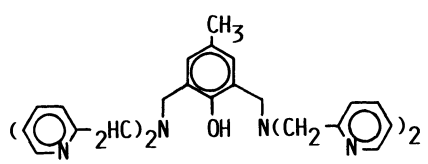

HL-py

Fig. 1. Dinucleating ligands (HL-Bzim): 2,6-bis[bis(2-benzimidazolylmethyl)aminomethyl]-4-methylphenol and (HL-py): 2,6-bis[bis(2-pyridylmethyl)aminomethyl]-4-methylphenol.

Experimental

Materials. HL-Bzim and HL-py were prepared as previously described.[15,16] $Fe(BF_4)_2\cdot 6H_2O$ was prepared by the know method.[17] The other chemicals were of reagent grade.

Preparation of Iron(II,III) Complexes. $[Fe_2(L\text{-}Bzim)(RCOO)_2](BF_4)_2\cdot nH_2O$ (RCOO=CH_3COO (**1**) or C_6H_5COO (**2**)): A solution of $Fe(BF_4)_2\cdot 6H_2O$ (2 mmol) in 20 cm^3 of ethanol was added with stirring to a solution of HL-Bzim (1 mmol), RCOOH (2 mmol), and triethylamine (1 mmol) in 20 cm^3 of ethanol under N_2. The resulting pale brown solution was exposed to air to form dark brown solution,

which was allowed to stand for a few hours at room temperature to give greenish brown crystals. They were filtered off, washed with ethanol and ether, and dried in vacuo. The complexes were recrystallized from acetonitrile–diethyl ether.

[Fe_2(L-Bzim)(C_6H_5COO)$_2$(OH)]$BF_4\cdot H_2O$ (3): A solution of $Fe(BF_4)_2\cdot 6H_2O$ (2 mmol) in 20 cm^3 of ethanol was added to an ethanol solution (20 cm^3) of HL-Bzim (1 mmol), C_6H_5COOH (1 mmol), and triethylamine (3 mmol) with stirring. The solution was exposed to air at 10 °C. The color changed to violet instantaneously. The violet solution was allowed to stand for several hours to give violet crystals, which were filtered off, washed with ethanol and ether, and dried in vacuo.

Preparation of Iron(III,III) Complexes. [Fe_2(L-Bzim)-(CH_3COO)$_2$](ClO_4)$_3\cdot 3.5H_2O$ (4): A solution of $Fe(ClO_4)_3$-$9H_2O$ (2 mmol) in 30 cm^3 of ethanol was mixed with a solution of HL-Bzim (1 mmol) and CH_3COONH_4 (2 mmol) in 20 cm^3 of ethanol with stirring. The resulting reddish brown solution was allowed to stand for several hours to give reddish brown crystals, which were collected by filtration, washed with ethanol and ether, and dried in vacuo.

[Fe_2(L-py)(C_6H_5COO)$_2$](ClO_4)$_3\cdot CH_3CN\cdot H_2O$ (5): A solution of $Fe(ClO_4)_3\cdot 9H_2O$ (2 mmol) in 20 cm^3 of acetonitrile was added to a solution of HL-Bzim (1 mmol), C_6H_5COOH (2 mmol), and triethylamine (2 mmol) in 30 cm^3 of ethanol. The resulting dark green solution was allowed to stand overnight to give dark green crystals, which were collected by filtration, washed with ethanol and ether, and dried in vacuo.

Analyses of iron(II) and iron(III) ions in the mixed valence complexes were carried out by the same method as that described in the literature.[11] The results are given in Table 1.

Measurements. The electronic spectra were measured on a Jasco UVIDEC 505 UV/VIS recording digital spectrophotometer and a Hitachi U-3400 spectrophotometer. Infrared spectra were obtained by the KBr-disk and Nujol mull methods with a Jasco A-3 infrared spectrophotometer. Magnetic susceptibilities were measured with a Shimadzu torsion magnetometer MB-2 which was calibrated with Hg[Co(NCS)$_4$]. Diamagnetic correction was made by using Pascal's constants.[18] Cyclic voltammograms were obtained with a Hokuto Denko HA-301 Potentiostat/Galvanostat and a Hokuto Denko HB-104 Function Generator in a cell containing a glassy carbon working electrode, a platinum-coil auxiliary electrode, and a saturated calomel electrode as reference electrode. Acetonitrile was used as the solvent and tetrabutylammonium perchlorate as the supporting electrolyte. Ferrocene was added for an internal check of redox potential and reversibility. $E_{1/2}$ of ferrocene was 0.39 V (vs. SCE) with a peak-to-peak separation (ΔE=70 mV). Mössbauer spectra were measured at 77 K against a ^{57}Co(Pt) source moving in a mode of constant acceleration. Velocity calibration was carried out by the resonance lines of metallic iron, and isomer shifts were given relative to iron metal at room temperature. The spectra of the mixed valence complexes were analyzed with a least square fitting program of Lorenztian functions into two sets of quadrupole doublets, each of which was fitted with an equal line width and intensity. ESR spectra were measured on a JEOL JES-FE2XG ESR spectrometer (X-band microwave unit, 100 KHz field modulation) equipped with an Air Product LTD-3-110 liquid helium transfer system. The microwave frequency was monitored with a Takeda Riken TR5212 microwave counter, and the resonance magnetic field values of the signals were measured with an NMR field meter (ECHO Electronics Co., Ltd.).

Results and Discussion

Characterization of Complexes. Chemical analyses of iron(II) and iron(III) ions in the complexes **1**, **2**, and **3** revealed that the complexes contain iron(II) and iron(III) ions in equimolar ratio. Mössbauer spectra also support the chemical analyses (vide infra). The molar conductivity of **1** in acetonitrile is 227 Ω^{-1} cm^2 mol^{-1}, characteristic of an 1:2 electrolyte. From the dinucleating nature of L-Bzim and the elemental analyses as well as the molar conductivities, the complexes **1** and **2** are formulated as [Fe_2(L-Bzim)($RCOO$)$_2$](BF_4)$_2\cdot nH_2O$ ($RCOO$=CH_3COO or C_6H_5COO). Recently Jameson et al. determined the crystal structure of [Fe_2(L-Bzim)(C_6H_5COO)$_2$](BF_4)$_2\cdot$ 2[$CF_3SO_3HN(C_2H_5)_3$] where two iron ions are triply bridged by phenolato and two benzoato bridges in syn–syn configuration.[19] Such triply bridging structure has been found for similar mixed valence iron(II, III) and manganese(II, III) complexes.[12,20,21]

The complex **3** was also isolated by treating the complex **2** with one equivalent of triethylamine; the addition of base to the acetonitrile–ethanol (1:1) solution of **2** resulted in an instantaneous color change from brown to reddish violet. When diethyl ether was

Table 1. Analytical Data of the Complexes

No.	Complex	Found (Calcd) (%)				
		C	H	N	Fe(II)	Fe(III)
1	[Fe_2(L-Bzim)(CH_3COO)$_2$](BF_4)$_2\cdot 2H_2O$	47.67 (48.03)	3.96 (4.21)	12.44 (12.45)	4.9 (4.97)	5.1 (4.97)
2	[Fe_2(L-Bzim)(C_6H_5COO)$_2$](BF_4)$_2\cdot 3H_2O$	51.87 (52.12)	4.12 (4.21)	11.12 (11.05)	4.2 (4.41)	4.4 (4.41)
3	[Fe_2(L-Bzim)(C_6H_5COO)$_2$(OH)]$BF_4\cdot H_2O$	56.52 (56.87)	4.20 (4.34)	11.93 (12.06)	4.7 (4.81)	5.0 (4.81)
4	[Fe_2(L-Bzim)(CH_3COO)$_2$](ClO_4)$_3\cdot 3.5H_2O$	42.23 (42.33)	3.74 (3.95)	11.17 (11.09)		9.0 (8.87)
5	[Fe_2(L-py)(C_6H_5COO)$_2$](ClO_4)$_3\cdot CH_3CN\cdot H_2O$	47.48 (47.42)	4.14 (3.90)	7.76 (7.90)		8.9 (9.00)

added to this solution under an inert atmosphere, violet crystals were obtained. Thus basic conditions are necessary for the formation of **3**. The conductivity measurement in DMF (66 Ω^{-1} cm^2 mol^{-1}) revealed that the complex is an 1:1 electrolyte. From the above results, it seems reasonable that the complex contains hydroxide ion and is formulated as $[Fe_2(Bzim)(C_6H_5COO)_2(OH)]BF_4\cdot H_2O$. At the present stage, however, the structure of **3** is not clear. The iron(III,III) complexes **4** and **5** also seem to have a triply bridging unit consisting of phenolato and two carboxylato bridges.

Magnetism. The effective magnetic moments of the mixed valence complexes **1**, **2**, and **3** at room temerature are all 7.7 B.M./Fe_2 and those of the iron(III,III) complexes **4** and **5** are 5.1 and 4.8 B.M./Fe, respectively. These values indicate that all the iron(II) and (III) ions are in high-spin state. Magnetic susceptivilities of the complexes were analyzed by the usual spin-spin interaction model based on exchange Hamiltonian $\mathscr{H}=-2JS_1\cdot S_2$. The molar susceptibilities (χ_A) of spin coupling dimers, (S_1=2, S_2=5/2), and (S_1=5/2, S_2=5/2) are given in Eqs. 1 and 2, respectively.

$$\chi_A=\frac{N\beta^2g^2}{4kT}\cdot\frac{x^{24}+10x^{21}+35x^{16}+84x^9+165}{x^{24}+2x^{21}+3x^{16}+4x^9+5} \quad (1)$$

$$\chi_A=\frac{2N\beta^2g^2(1-P)}{kT}\cdot\frac{x^{28}+5x^{24}+14x^{18}+30x^{10}+55}{x^{30}+3x^{28}+5x^{24}+7x^{18}+9x^{10}+11}+\frac{4.34P}{T} \quad (2)$$

where x=exp($-J/kT$), the symbols have usual meanings, and temperature independent paramagnetisms ($N\alpha$) are assumed to be zero. The magnetic susceptibilities of the iron(II,III) and iron(III,III) complexes were interpreted in terms of the above equations with the parameters listed in Table 2 (Fig. 2). These results indicate that high-spin iron(II) and iron(III) ions in the iron(II, III) complexes are weakly antiferromagnetically coupled to yield an S=1/2 spin ground state. The iron (III, III) complexes also exhibit weak antiferromagnetic exchange interacrion to yield an S=0 spin ground state. Analogous mixed valence dinuclear iron(II,III) and manganese(II,III) complexes with phenolato and two carboxylato bridges show comparable magnitude of antiferromagnetic interaction (J=−3——8 cm^{-1}).[11,20,21] Thus phenolato and carboxylato bridges seem to provide weak antiferromagnetic interaction for all the iron and manganese dinuclear systems, regardless of homoval-ent or mixed valent system.

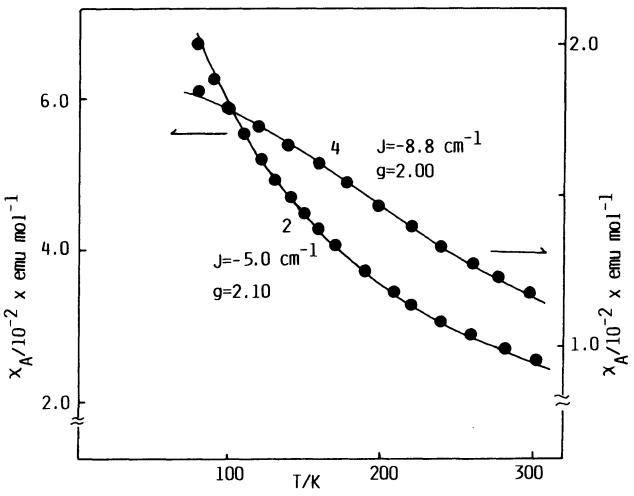

Fig. 2. Temperature dependence of magnetic susceptibilities of $[Fe_2(L\text{-}Bzim)(C_6H_5COO)_2](BF_4)_2\cdot 3H_2O$ (**2**) and $[Fe_2(L\text{-}Bzim)(CH_3COO)_2](ClO_4)_3\cdot 3.5H_2O$ (**4**).

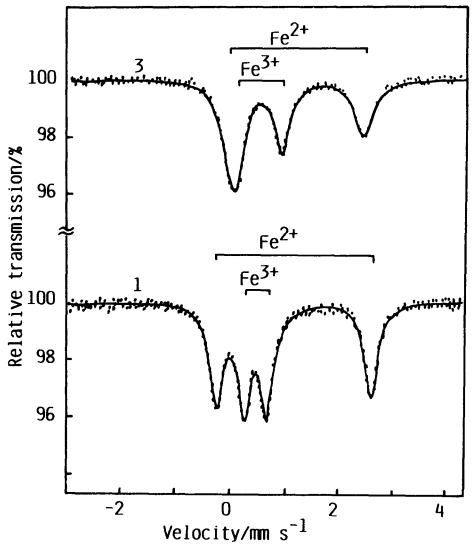

Fig. 3. Mössbauer spectra of $[Fe_2(L\text{-}Bzim)(CH_3COO)_2]\cdot(BF_4)_2\cdot 2H_2O$ (**1**), and $[Fe_2(L\text{-}Bzim)(C_6H_5COO)_2(OH)]\cdot BF_4\cdot H_2O$ (**3**) at 77 K.

Table 2. Magnetic Parameters of the Complexes[a]

No.	Complex	J/cm^{-1}	g
1	$[Fe_2(L\text{-}Bzim)(CH_3COO)_2](BF_4)_2\cdot 2H_2O$	−5.0	2.10
2	$[Fe_2(L\text{-}Bzim)(C_6H_5COO)_2](BF_4)_2\cdot 3H_2O$	−5.0	2.10
3	$[Fe_2(L\text{-}Bzim)(C_6H_5COO)_2(OH)]BF_4\cdot H_2O$	−4.0	2.10
4	$[Fe_2(L\text{-}Bzim)(CH_3COO)_2](ClO_4)_3\cdot 3.5H_2O$	−8.8	2.00
5	$[Fe_2(L\text{-}py)(C_6H_5COO)_2](ClO_4)_3\cdot CH_3CN\cdot H_2O$[b]	−12.0	2.00

a) $N\alpha$ is assumed to be zero. b) Fitted with contamination of 2% of monomeric high-spin iron(III) impurity.

Table 3. Mössbauer Parameters of the Complexes at 77 K[a)]

No.	Complex	Fe(II)			Fe(III)			A(Fe(III)/Fe(II))[c)]
		δ[b)]	ΔE	Γ	δ[b)]	ΔE	Γ	
1	$[Fe_2(L\text{-}Bzim)(CH_3COO)_2](BF_4)_2\cdot 2H_2O$[d)]	1.29	2.81	0.28	0.58	0.40	0.30	1.11
2	$[Fe_2(L\text{-}Bzim)(C_6H_5COO)_2](BF_4)_2\cdot 3H_2O$[d)]	1.18	2.15	0.37	0.56	0.96	0.40	1.10
3	$[Fe_2(L\text{-}Bzim)(C_6H_5COO)_2(OH)]BF_4\cdot H_2O$[d)]	1.29	2.45	0.37	0.61	0.81	0.32	1.06
4	$[Fe_2(L\text{-}Bzim)(CH_3COO)_2](ClO_4)_3\cdot 3.5H_2O$[d)]				0.27	0.71	0.59	
	$[Fe_2(L\text{-}py)(CH_3COO)_2](BF_4)_2\cdot 2H_2O$[e)]	1.16	2.42	0.41	0.47	0.51	0.33	
	$[Fe_2(L\text{-}py)(C_6H_5COO)_2](BF_4)_2\cdot 2H_2O$[e)]	1.15	2.06	0.56	0.56	0.47	0.27	

a) All data in mm s^{-1} except for A(Fe(III)/Fe(II)). b) Isomer shift, δ, relative to iron metal. c) Ratios of areas of Fe(III) to Fe(II). d) This work. e) Ref. 11.

Mössbauer Spectra. Mössbauer spectra of **2** and **3** are given in Fig. 3 and their parameters are listed in Table 3. The presence of iron(II) and iron(III) ions in equimolar ratio in mixed valence complexes is evidenced by the fact that the ratios of area of two sets of quadrupole doublets are nearly unity (Table 3). This fact agrees with the results of the chemical analyses. The quadrupole splitting ΔE and isomer shift δ in mm s^{-1} of the mixed valence complexes are 2.15—2.81 and 1.18—1.29 for iron(II) moieties, and 0.40—0.96 and 0.56—0.61 for iron(III) moieties, respectively. The former quadrupole splitting and isomer shift fall in the range of those of the high spin iron(II) complexes and the latters in the range of iron(III) complexes, respectively.[22)] Although the structure of **1** and **2** seem to be almost identical, the quadrupole splittings of the iron(II) and iron(III) moieties in **1** and **2** significantly differ from each other. The iron(II) moiety of **1** exhibits a larger ΔE (2.81) than that of **2** (2.15), whereas the iron(III) moiety of **2** exhibits a larger ΔE (0.96) than that of **1** (0.40). A larger quadrupole splitting reflects a larger electric field gradient at the nucleus, suggesting a lower symmetry of ligand field; i.e., the distortion from octahedron in iron(II) moiety of **1** is larger than that of **2**, but this relation is reversed for iron(III) moieties. The quadrupole splittings of iron(II) and iron(III) moieties in the acetato and benzoato complexes with L-py are 2.42 and 2.06, and 0.51 and 0.47 mm s^{-1}, respectively, suggesting that structural difference between acetato and benzoato complexes with L-py is smaller than that between the L-Bzim complexes and a distortion from octahedron in the L-Bzim complexes is larger than that in L-py complexes. For further discussion, structural details are necessary.

ESR Spectra. All the ESR spectra of the mixed valence complexes in frozen glass of acetonitrile solution as well as in the polycrystalline phase (Fig. 4) show a broad signal at $g\approx 1.7$ at 12 K, indicative of the existence of dinuclear high-spin iron(II,III) mixed valence center where iron(II) and (III) ions are antiferromagnetically coupled to yield a spin ground state of $S=1/2$. The $g\approx 1.7$ signals are observable only near liguid helium temperature and almost disappear above 30 K. Such a spectral behavior is very similar to

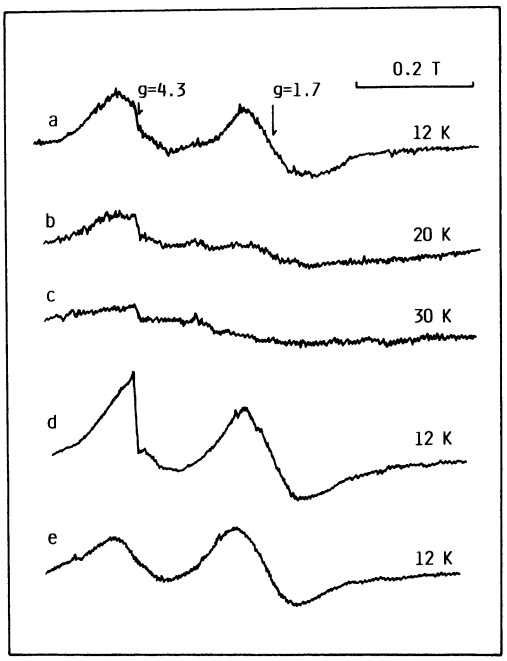

Fig. 4. ESR spectra of $[Fe_2(L\text{-}Bzim)(C_6H_5COO)_2](BF_4)_2\cdot 3H_2O$ (**2**) at 12 K (a), 20 K (b), and 30 K (c) in acetonitrile, and $[Fe_2(L\text{-}Bzim)(C_6H_5COO)_2(OH)]BF_4\cdot H_2O$ (**3**) at 12 K (d) in acetonitrile and at 12 K (e) in polycrystalline phase.

those of the mixed valence iron proteins such as semimethemerythrin[8)] and the L-py complexes,[11)] although the signal of the present complexes is very broad as compared with those of the iron proteins. All the frozen solution spectra exhibit a sharp signal at $g\approx 4.3$ attributable to a mononuclear rhombic high-spin iron(III) complex present as impurity formed by slight decomposition in solution. In fact, the spectrum of **3** in polycrystalline phase has no such signal at $g\approx 4.3$. It should be noted that in all the present mixed valence complexes there is a broad signal at $g\approx 5$—6 which is absent in the iron proteins and the L-py complexes.[11)] As illustrated in Fig. 4a, b, and c, the $g\approx 5$—6 signals also show a temperature dependence which is similar to that at $g\approx 1.7$. The signals at $g\approx 5$—6 may be ascribed to the complex in $S=3/2$ spin state. The mixed valence manganese(II, III) complexes also have such a broad signal at $g\approx 4$.[20,21)]

Table 4. Electronic Spectral Data of the Complexes[a)]

No.	Complex	ν_{max}/cm^{-1}, (ε/mol^{-1} dm^3 cm^{-1}) CT band	IT band	
1	$[Fe_2(L\text{-}Bzim)(CH_3COO)_2](BF_4)_2\cdot 2H_2O$[d)]	19200(940)[s]	7400(230)	10300[s]
2	$[Fe_2(L\text{-}Bzim)(C_6H_5COO)_2](BF_4)_2\cdot 3H_2O$[d)]	18500(880)[s]	7040(220)	10200[s]
3	$[Fe_2(L\text{-}Bzim)(C_6H_5COO)_2(OH)]BF_4\cdot H_2O$[d)]	18520(3200)	8000(200)[b)]	
4	$[Fe_2(L\text{-}Bzim)(CH_3COO)_2](ClO_4)_3\cdot 3.5H_2O$[d)]	21740(4120) 19800(2060)[c)]		
5	$[Fe_2(L\text{-}py)(C_6H_5COO)_2](ClO_4)_3\cdot CH_3CN\cdot H_2O$[d)]	16950(920)		
	$[Fe_2(L\text{-}py)(CH_3COO)_2](BF_4)_2\cdot H_2O$[e)]	18000(900)	7700(290)	
	$[Fe_2(L\text{-}py)(C_6H_5COO)_2](BF_4)_2\cdot 2H_2O$[e)]	17400(970)	7400(290)	

a) In acetontrile under N_2. b) Broad band. c) In DMF. d) This work. e) Ref. 11. s: Shoulder.

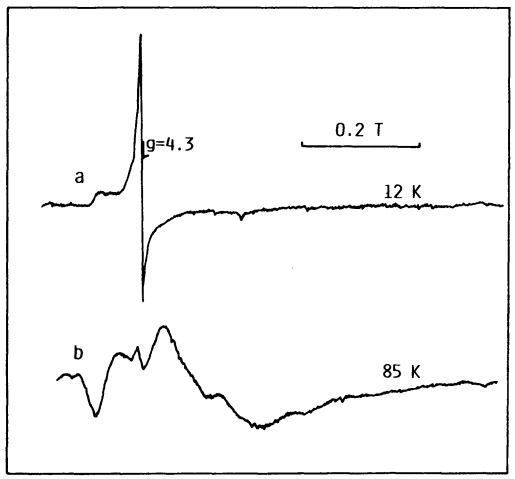

Fig. 5. ESR spectra of $[Fe_2(L\text{-}py)(C_6H_5COO)_2](ClO_4)_3\cdot CH_3CN\cdot H_2O$ (**5**) at 12 K (a) and at 85 K (b) in acetonitrile.

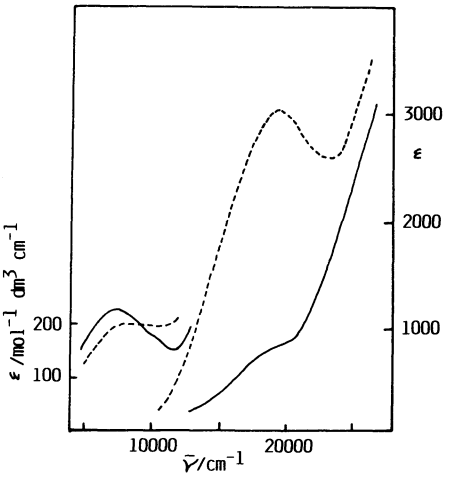

Fig. 6. Electronic spectra of $[Fe_2(L\text{-}Bzim)(C_6H_5COO)_2](BF_4)_2\cdot 3H_2O$ (**2**) (——) and $[Fe_2(L\text{-}Bzim)(C_6H_5COO)_2(OH)]BF_4\cdot H_2O$ (**3**) (------) in acetonitrile under nitrogen atmosphere.

The ESR spectrum of **5** is illustrated in Fig. 5. A significant temperature dependence is observed in the spectra. The spectral behavior of **4** is very similar to that of **5**. They have six spin states of S=0, 1, 2, 3, 4, and 5, in which an S=0 state is the lowest. The spectrum at 12 K exhibits an intense signal at $g\approx 4.3$ and weaker one at higher g values which are attributable to mononuclear iron(III) impurity. Since at 12 K, the population in the ESR active states (S=1, 2, 3, 4, and 5) is about 14%, which was estimated on the basis of Boltzmann distribution by using $J=-12$ cm^{-1}, the signals would be expected to be very weak. On the other hand, at 85 K the population of those states becomes larger (S=0: 19%, S=1: 38%, S=2: 28%, S=3: 11%, S=4: 3%, S=5: 1%) and signals would be expected. In fact, several broad and complicated signals are observed at 85 K (Fig. 5). Such complex spectra were also reported for dinuclear complexes.[23,24)]

Electronic Spectra. The electronic spectra of the mixed valence complexes exhibit an absorption band in the near infrared region (ε=200 mol^{-1} dm^3 cm^{-1}/Fe_2) in acetonitrile (Fig. 6 and Table 4), whereas no such band is observed in this region for the iron(III, III) complexes. The analogous iron(II, III) complexes with L-py also have a near infrared band. Such bands can be assigned to the intervalence transition (IT) of the type $[Fe^{2+}\text{-}Fe^{3+}]\xrightarrow{h\nu}[Fe^{3+}\text{-}Fe^{2+}]^*$. All the complexes have an IT band with a shoulder at higher energy side, while the L-py complexes exhibit only a single IT band. The presence of shoulder may reflect a splitting of t_{2g} orbitals of iron(III) moiety resulting from a lower ligand field symmerty.

All the mixed valence complexes have a charge-transfer transition (CT) from bridging phenolato group to iron(III) moiety in the visible region. The molar extinction coefficients of the CT bands in **1** and **2** are ca. 900 mol^{-1} dm^3 cm^{-1}, whereas that of **3** is 3200 mol^{-1} dm^3 cm^{-1}. The CT band of the iron(III, III) complex **4** showed a remarkable solvent effect (Table 4); the CT band appeared at 21740 cm^{-1} (ε=4120 mol^{-1} dm^3 cm^{-1}) in acetonitrile, and at 19800 cm^{-1} (ε=2060 mol^{-1} dm^3 cm^{-1}) in DMF. Thus such significant energy and intensity variations of the CT band may reflect some structural change in the phenolato bridge.

Ainscough et al.[25)] and Pyrz et al.[26)] pointed out that for mononuclear iron(III)-phenolate complexes the energy of CT band of phenolate moiety to iron(III) ion is sensitive to the donor strength of the other ligands

Table 5. Cyclic Voltammetric Data of the Mixed Valence Complexes

No.	Complex	$E_{1/2}$[a] (E/V vs. SCE)	$E_{1/2}$[b]	(i_{pa}/i_{pc})[a]	(i_{pa}/i_{pc})[b]	K_c
1	$[Fe_2(L\text{-}Bzim)(CH_3COO)_2](BF_4)_2\cdot 2H_2O$[e]	−0.12	+0.56	1.2	1.1	5.0×10^{11}
2	$[Fe_2(L\text{-}Bzim)(C_6H_5COO)_2](BF_4)_2\cdot 3H_2O$[e]	0.00	+0.66	1.1	0.9	2.2×10^{11}
3	$[Fe_2(L\text{-}Bzim)(C_6H_5COO)_2(OH)]BF_4\cdot H_2O$[e]	−0.16	+0.28			
	$[Fe_2(L\text{-}py)(CH_3COO)_2](BF_4)_2\cdot H_2O$[f]	−0.03	+0.68			1.6×10^{12}
	$[Fe_2(L\text{-}py)(C_6H_5COO)_2](BF_4)_2\cdot 2H_2O$[f]	+0.05	+0.73			5.0×10^{11}

a) For Fe(II,III)/Fe(II,II) redox couple. b) Fe(III,III)/Fe(II,III) redox couple. c) Comproportionation constant at 20 °C. d) Irreversible. e) This work. f) Ref. 11.

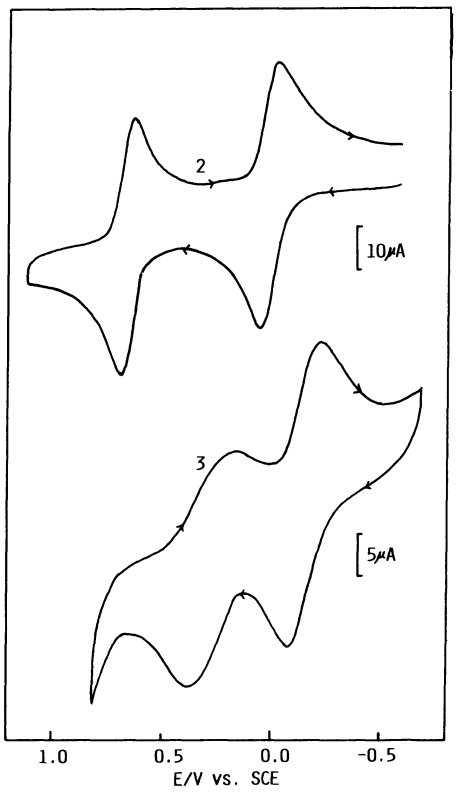

Fig. 7. Cyclic voltammograms of $[Fe_2(L\text{-}Bzim)(C_6H_5COO)_2](BF_4)_2\cdot 3H_2O$ (**2**) and $[Fe_2(L\text{-}Bzim)(C_6H_5COO)_2(OH)]BF_4\cdot H_2O$ (**3**) in 0.1 mol dm^3 tetrabutylammonium perchlorate in acetonitrile at a glassy carbon electrode at a scan rate of 100 mV s^{-1}.

coordinated and the redox potential of the complex; i.e., the donor strength of the other ligands becomes stronger, the more negative the redox potential and the higher the energy of the charge-transfer transition. The present iron(II, III) and (III, III) complexes have a charge-transfer band at higher energy region than the corresponding L-py complexes and the redox potentials of the L-Bzim complexes are more negative than those of the L-py complexes (vide infra). This observation implies that the benzimidazolyl group of L-Bzim is a stronger donor than the pyridyl group of L-py.

Cyclic Voltammogram. Figure 7 illustrates the cyclic voltammograms of **2** and **3** in acetonitrile (Table 5). The complex **2** shows two reversible redox couples at +0.00 and +0.66 V vs. SCE, which correspond to the redox reactions of Fe(II,III)/Fe(II,II) and Fe(III, III)/Fe(II,III). A similar CV was observed for **1**. The redox potentials of **1** and **2** are more negative by 50—120 mV than those of the corresponding L-py complexes. Such negative shifts are consistent with the shift of the CT band energies of the L-Bzim and L-py complexes. The CV of **3** also exhibits two redox couples at ca. −0.16 and +0.28 V vs. SCE, although the reversibility is poor as compared with those of **1** and **2**. Introduction of hydroxide ion seems to cause a poor reversibility and negative shift. A similar situation was obseved for the L-py complexes.[11]

Comproportionation constants of **1** and **2** in the following equilibrium are $5—2\times10^{11}$, indicating that the mixed valence

$$Fe(II, II) + Fe(III, III) \rightleftharpoons 2Fe(II, III)$$

complexes are significantly stabilized. Thus, the present ligand system (L-Bzim and two carboxylato) also provides favorable coordination sites toward M^{2+} and M^{3+} ions to form a mixed valence complex as the L-py ligand system (L-py and two carboxylate ions) does.

References

1) L. Que, Jr., *Coord. Chem. Rev.*, **50**, 73 (1983).
2) B. C. Antanaitis and P. Aisen, *Adv. Inorg. Biochem.*, **5**, 111 (1983).
3) B. C. Antanaitis, P. Aisen, and H. E. Lilienthal, *J. Biol. Chem.*, **258**, 3166 (1983).
4) R. B. Lauffer, B. C. Antanaitis, P. Aisen, and L. Que, Jr., *J, Biol. Chem.*, **258**, 14212 (1983).
5) P. G. Debrunner, M. P. Hendrich, J. D. Jersey, D. T. Keough, J. T. Sage, and B. Zerner, *Biochim. Biophys. Acta*, **745**, 103 (1983).
6) J. C. Davis and B. A. Averill, *Proc. Natl. Acad. Sci. U.S.A.*, **79**, 4623 (1982).
7) R. G. Wilkins and P. C. Harrington, *Adv. Inorg. Biochem.*, **5**, 51 (1983).
8) B. B. Muhoberac, D. C. Wharton, L. M. Babcock, P. C. Harrington, and R. G. Wilkins, *Biochim. Biophys. Acta*, **626**, 337 (1980).
9) D. M. Kurtz, Jr., J. T. Sage, M. Hendrich, P. G. Debrunner, and G. S. Lukat, *J. Biol. Chem.*, **258**, 2115 (1983).

10) M. Suzuki, A. Uehara, and K. Endo, *Inorg. Chim. Acta*, **123**, L9 (1986).
11) M. Suzuki, A. Uehara, H. Oshio, K. Endo, M. Yanaga, S. Kida, and K. Saito, *Bull. Chem. Soc. Jpn.*, **60**, 3547 (1987).
12) A. S. Brovik and L. Que, Jr., *J. Am. Chem. Soc.*, **110**, 2345 (1988).
13) A. S. Borovik, B. P. Murch, and L. Que, Jr., *J. Am. Chem. Soc.*, **109**, 7190 (1987).
14) J. R. Hartman, R. L. Rardin, P. Chaudhuri, K. Pohl, K. Wieghardt, B. Nuber, J. Weiss, G. C. Papaefthymiou, R. B. Frankel, and S. J. Lippard, *J. Am. Chem. Soc.*, **109**, 7387 (1987).
15) M. Suzuki, H. Kanatomi, and I. Murase, *Chem. Lett.*, **1981**, 1745.
16) M. Suzuki, H. Kanatomi, and I. Murase, *Bull. Chem. Soc. Jpn.*, **57**, 36 (1984).
17) C. L. Spiro, S. L. Lambert, T. J. Smith, E. N. Duesler, R. R. Gagné, and D. N. Hendrickson, *Inorg. Chem.*, **20**, 1229 (1981).
18) F. E. Mabbs and D. J. Marchin "Magnetisms and Transition Metal Complexes," Chapman and Hall, London (1975), p. 5.
19) A. B. Hussein, N. L. Morris, P. G. Romero, and G. B. Jameson, private communication.
20) a) M. Suziki, S. Murata, A. Uehara, and S. Kida, *Chem Lett.*, **1987**, 281; b) M. Suzuki, M. Mikuriya, S. Murata, A. Uehara, H. Oshio, S. Kida, and K. Saito, *Bull. Chem. Soc. Jpn.*, **60**, 4305 (1987).
21) H. Diril, H. R. Chang, X. Zhang, S. K. Larsen, J. A. Potenza, C. G. Pierpont, H. J. Schugar, S. S. Isied, and D. N. Hendrickson, *J. Am. Chem. Soc.*, **109**, 6207 (1987).
22) N. N. Greenwood and G. T. Gibbs, "Mössbauer Spectroscopy," Chapman and Hall, London (1971), p. 148.
23) R. G. Wollmann and D. N. Hendrickson, *Inorg. Chem.*, **17**, 926 (1978).
24) E. W. Aniscough, A. M. Brodie, and S. J. McLachlan, *J. Chem. Soc., Dalton Trans.*, **1983**, 1385.
25) E. W. Aniscough, A. M. Brodie, J. E. Plowman, K. L. Brown, A. W. Addison, and A. R. Gainsford, *Inorg. Chem.*, **19**, 3655 (1980).
26) J. W. Pyrz, A. L. Roe, L. J. Stern, and L. Que, Jr., *J. Am. Chem. Soc.*, **107**, 614 (1985).